No attenuation of fish and mammal biodiversity declines in the Guiana Shield

Article *in* The Science of The Total Environment · March 2025

DOI: 10.1016/j.scitotenv.2025.179021

8 authors, including:

Opale Coutant
Laboratory Evolution and Biological Diversity
16 PUBLICATIONS **191** CITATIONS
SEE PROFILE

Manuel Lopes-Lima
University of Porto
310 PUBLICATIONS **6,327** CITATIONS
SEE PROFILE

Loïc Pellissier
ETH Zurich/ WSL Birmensdorf
326 PUBLICATIONS **15,753** CITATIONS
SEE PROFILE

Grégory Quartarollo
Hydreco
3 PUBLICATIONS **11** CITATIONS
SEE PROFILE

Science of the Total Environment 971 (2025) 179021

Contents lists available at ScienceDirect

Science of the Total Environment

journal homepage: www.elsevier.com/locate/scitotenv

No attenuation of fish and mammal biodiversity declines in the Guiana Shield

Opale Coutant [a,*], Manuel Lopes-Lima [b], Jérôme Murienne [a], Loic Pellissier [c,d], Grégory Quartarollo [e,f], Alice Valentini [g], Vincent Prié [g,1], Sébastien Brosse [a,1]

[a] Centre de Recherches sur la Biodiversité et l'Environnement, CRBE UMR5300, Université de Toulouse, IRD, CNRS, INP 118 route de Narbonne, 31062 Toulouse, France
[b] Centro de Investigação em Biodiversidade e Recursos Genéticos, CIBIO, InBIO Laboratório Associado, at the Universidade do Porto, in Vairão, Portugal
[c] Ecosystems and Landscape Evolution, Department of Environmental Systems Science, ETH Zürich, Zürich, Switzerland
[d] Land Change Science Research Unit, Swiss Federal Institute for Forest, Snow and Landscape Research (WSL), Birmensdorf, Switzerland
[e] HYDRECO, Laboratoire Environnement de Petit Saut, Kourou, French Guiana
[f] Guyane Wild Fish, Cayenne, French Guiana
[g] SPYGEN, Le Bourget-du-Lac, France

HIGHLIGHTS

- Real-time biodiversity monitoring captures progressive shifts in ecological communities.
- Short-term spatiotemporal changes in vertebrate communities were monitored using eDNA in Northern Amazonia.
- Slight anthropogenic disturbances over four years caused taxonomic and functional modifications.
- Mammal and fish communities experienced declines in extreme functional strategies.
- The overall magnitude of biodiversity decline continued at the same pace over four years.

GRAPHICAL ABSTRACT

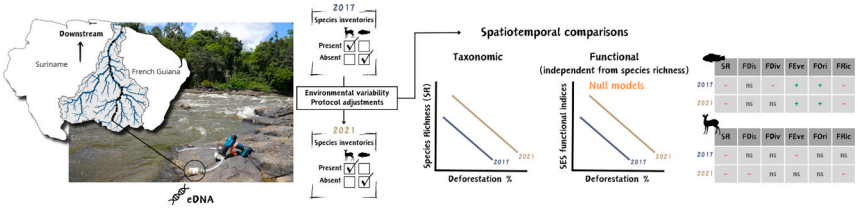

ARTICLE INFO

Editor: Shuqing Zhao

Keywords:
Fish
Mammals
Deforestation
Taxonomic
Functional
eDNA

ABSTRACT

Real-time biodiversity monitoring should provide more resolved data to quantify shifts in ecological communities progressively altered by anthropogenic disturbances. Identifying biodiversity trends requires a rapid and efficient inventory method that enables the collection and delivery of high-resolution data within short intervals. Using aquatic environmental DNA (eDNA), we investigated spatiotemporal changes in fish and mammal communities along the Maroni River in French Guiana. We compared spatial biodiversity trends between two years, separated by a four-year interval, during which an increase in anthropogenic disturbances was observed. To evaluate biodiversity changes, we examined the impact of these disturbances on both taxonomic and functional diversity. Our findings revealed that, while the increase in disturbances did not result in major biodiversity decline, it continued to drive alterations in community taxonomic and functional richness. Communities

* Corresponding author.
E-mail addresses: opale.coutant@univ-tlse3.fr (O. Coutant), jerome.murienne@univ-tlse3.fr (J. Murienne), loic.pellissier@usys.ethz.ch (L. Pellissier), gregory.quartarollo@hydrecolab.com (G. Quartarollo), alice.valentini@spygen.com (A. Valentini), vincent.prie@spygen.com (V. Prié), sebastien.brosse@univ-tlse3.fr (S. Brosse).
[1] Co-senior authorship.

https://doi.org/10.1016/j.scitotenv.2025.179021
Received 8 November 2024; Received in revised form 30 January 2025; Accepted 27 February 2025
Available online 12 March 2025

underwent changes in their functional structure, with mammal communities experiencing a decline in extreme functional traits, while fish communities lost functional redundancy in generalist functions and experienced a reduction in extreme functional strategies. In a context of small-scale anthropogenic disturbances, these changes highlight the necessity of long-term, short-interval monitoring to capture rapid reorganisation of ecological communities under stress.

1. Introduction

Current global biodiversity assessments reveal a steep decline in biodiversity across all ecosystems, with both freshwater and terrestrial vertebrates among the most imperiled (WWF, 2024). For these two groups, the Intergovernmental Platform for Biodiversity and Ecosystem Services (IPBES) reports increases in extinction rates since the beginning of the 20th century (IPBES, 2019) and recent studies highlight the role of global anthropogenic disturbances in driving these drastic changes worldwide (Matthews et al., 2024; Su et al., 2021). Deforestation is a primary driver of habitat loss in both terrestrial and freshwater ecosystems, reducing habitat heterogeneity by altering river morphology and water physicochemical parameters (Arantes et al., 2018; Brejão et al., 2018; Cantera et al., 2023a). Deforestation does not happen necessarily over broad area, but can occur as a continuous fragmentation of the continuous forest matrix into fragmented patches. As a results, the impact on the biodiversity can be in the form of a progressive erosion, but current monitoring methods have difficulties to highlight slow continuous trends.

In tropical regions such as the Amazonian Guiana Shield, deforestation stems primarily from mining activities, significantly impacting both terrestrial and freshwater ecosystems (Cantera et al., 2022; Dezécache et al., 2017). Mining activities alter sediment flux balances, leading to increased turbidity that affects photosynthetic processes, the production of dissolved oxygen, and the visibility of aquatic organisms. Environmental changes, in turn, impact foraging, reproduction, and the development of eggs and larvae in the case of fishes (Gallay et al., 2018). In terrestrial ecosystems, in addition to habitat loss and degradation, small-scale gold mining is often associated with subsistence hunting and poaching activities, which significantly affect large-bodied species (Cantera et al., 2022). Both ecosystems are linked together by complex ecological networks and trophic interactions, as well as by interdependent abiotic conditions (Sullivan and Manning, 2019; Zhang et al., 2023). Integrated terrestrial-freshwater conservation planning accounting for their lateral connectivity can double the conservation of tropical aquatic species (Leal et al., 2020). Given the continuous population declines reported in both realms (Carmona et al., 2021), real-time monitoring of the taxonomic and functional facets of fish and mammal communities is pivotal to understanding how composition is being modified by anthropogenic disturbances and to predict the long-term trajectories of these communities.

Compared to those global and long-term assessments of biodiversity trends, local and short-term evaluations of biodiversity changes remain limited, although they are essential for bending the curve of biodiversity decline (Tickner et al., 2020). The lack of short-term biodiversity follow-up is likely rooted in the complexity of gathering real-time inventories, which require labour-intensive fish catches (Keck et al., 2022) and time-intensive surveys for mammals (De Thoisy et al., 2008), especially in megadiverse regions. Sampling limitation has recently been addressed by the development of environmental metabarcoding technologies, which enable rapid and extensive local biodiversity assessments based on the collection of environmental DNA (eDNA) drained by rivers (Taberlet et al., 2018). This method has been demonstrated to be efficient to inventory local freshwater fish (Cantera et al., 2019; Cilleros et al., 2019; Yao et al., 2022) and terrestrial mammal faunas (Coutant et al., 2021; Lyet et al., 2021; Macher et al., 2021; Mena et al., 2021) worldwide. Short-term biodiversity follow-ups are particularly susceptible to biases that can affect biodiversity inventories, especially when compared to long-term monitoring. In contrast, long-term monitoring data collected over extended periods can allow to distinguish between background variabilities and long-term trends that accurately reflect ecological processes (Dale and Beyeler, 2001). Short-term fluctuations can arise from variability in environmental conditions or in the inventory methods, such as differences in sampling effort, the locations of samples, or protocol optimisation. eDNA methods are particularly subject to these biases. For example, wet seasons characterised by higher water levels may influence the transport and the decay rate of eDNA (Harrison et al., 2019; Pont, 2024). Meanwhile, eDNA-based methods are continually improving as we gain a better understanding of effective eDNA collection and processing, leading to necessary protocol adjustments (Coutant et al., 2020). Environmental variability and protocol adjustments, which introduce background variability in the data, raise questions about the relevance of eDNA methods for detecting short-term temporal variations in assemblages (Carraro et al., 2023; Mathieu et al., 2020).

Spatiotemporal biodiversity monitoring is particularly relevant in riverine ecosystems and associated terrestrial habitat, where anthropogenic activities are unevenly distributed along rivers and often intensify with river size (Pringle, 2001). Moreover, the impacts of human activities can vary depending on their location along the river continuum, as hydrological connectivity transports materials and sediments downstream, amplifying their influence (Pringle, 2001). Therefore, evaluating the spatial variation of species over time along the river longitudinal upstream-downstream gradient can help identify processes modifying species distribution across space. Measuring these changes in biodiversity requires considering both changes in species diversity (taxonomic diversity) as well as changes in the roles occupied by species (functional diversity) (Mouillot et al., 2013), with each facet potentially being affected differently by global changes (Coutant et al., 2023; Mouillot et al., 2013).

Here, we monitored 32 fish and mammal communities using aquatic eDNA during the dry seasons of 2017 and 2021 along the Maroni River in Northern Amazonia. Although the Maroni River basin is considered one of the world's best preserved basin (Su et al., 2021; Watson et al., 2018), it is currently facing unprecedented threats related to diverse anthropogenic activites.

Small-scale gold mining is the primary driver of deforestation, responsible for approximately 40 % of the deforested areas and severely impacting water quality and the river's physical structure (Cantera et al., 2022; Castello and Macedo, 2016). Other activities such as logging and slash-and-burn agriculture also take place along the river, contributing to deforestation. Based on eDNA data collected in 2017 on the Maroni River, Cantera et al. (2022) reported that both the taxonomic and functional diversity of fish and mammals were approximately 30 % lower in disturbed sites compared to undisturbed ones. Large uncertainties remain regarding biodiversity changes experienced by the Maroni River basin in recent years, as a significant portion of the basin is designated as a French national protected area while simultaneously being increasingly impacted by a gold mining rush triggered by rising gold prices (Dezécache et al., 2017). Unraveling the recent biodiversity trends in fish and mammals is therefore critical for the current and future management of this biodiversity hotspot. We investigated the spatiotemporal taxonomic and functional changes in fish and mammal assemblages in response to deforestation observed between 2017 and 2021, which serves as a surrogate for anthropogenic disturbances (Cantera et al., 2022). We tested whether taxonomic and functional

biodiversity changes were noticeable across the Maroni River basin within a four-year time frame (2017–2021), assessing the potential for rapid recovery or alteration of fish and mammal assemblages. We address the following questions: (i) Do fish and mammal communities exhibit different responses along the upstream-downstream gradient in 2021 compared to 2017? Since deforestation increased primarily in the middle and downstream sections of the river, we expect more pronounced temporal changes in communities in the downstream section in 2021 compared to those in the upstream section. (ii) What changes in functional diversity and structure characterise fish and mammal communities in 2017 compared to 2021? We expect that communities in 2021 will be characterised by a decline in functional diversity, along with shifts in functional structure, driven by the gradual replacement of specialist species by generalists. We expect reductions in functional richness, functional divergence, and functional evenness as already evidenced in the region in Cantera et al. (2023b).

2. Material and Method

2.1. Study area

We sampled biodiversity on the Maroni River located between French Guiana and Suriname, in the northeastern Amazonian biome (Fig. 1). The Maroni River is the main course (612 km from the source to the estuary) of the Maroni basin covering a surface of ±68,000 km^2 in Suriname and French Guiana. The climate of the entire study area is relatively homogeneous and the region is covered by dense, uniform lowland primary rainforest. The elevation is in the range of 0–860 m a.s.l. The regional climate is equatorial, and the annual rainfall ranges from 2000 mm in the southwest to 3600 mm in the northeast. The Maroni river is inhabited by *c.* 83,000 people (INSEE, 2020), unevenly distributed from Saint-Laurent du Maroni to the village of Pidima, which constitutes the most upstream human settlement on the Maroni river (Fig. 1). The river faces the highest rate of deforestation of the territory and is also the most affected by illegal gold mining, spanning from Saint-Laurent du Maroni to upstream of Maripasoula (Gallay et al., 2018). Only the most upstream part of the Maroni River (upstream of Pidima, Fig. 1) is not impacted by human activities.

Despite the same monitoring season in November 2017 and 2021, both years were characterised by distinct environmental conditions. The year 2017 was the 5th warmest since 1955, with a dry season characterised by a 13 % deficit in precipitation compared to the reference period of 1981–2010. In contrast, the year 2021 was distinguished by markedly elevated precipitation levels (annual cumulative precipitation 41 % higher than the reference period 1981–2010). The rainy season started with three weeks advance and the pluviometry of November presented an excess rainfall of 62 % (Météo France, 2024; Fig. 1). Therefore, despite identical sampling dates in the 2017 and 2021 field

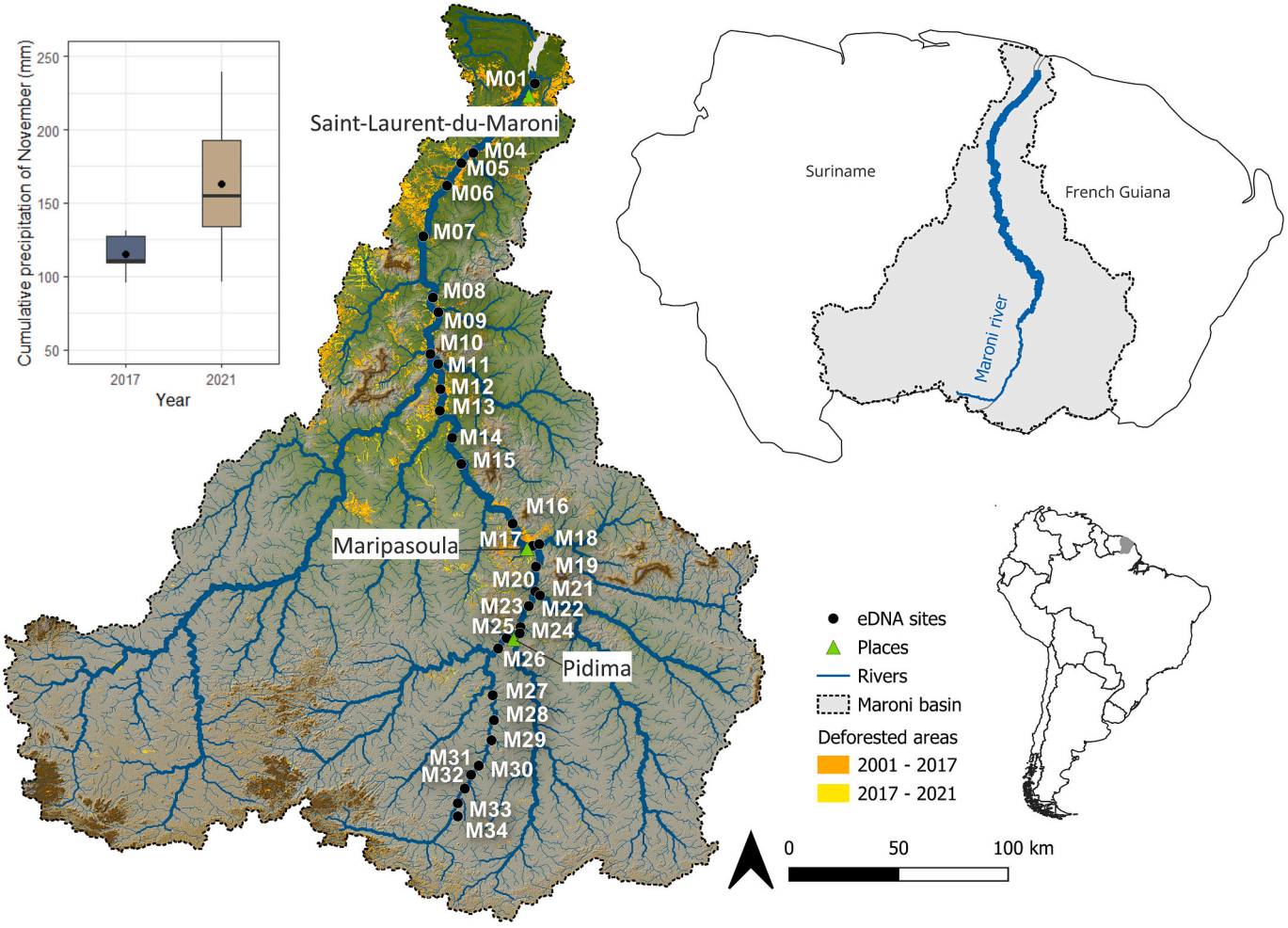

Fig. 1. Map of the study area and the 32 eDNA sites surveyed in 2017 and 2021. The inset map in the bottom right corner indicates the location of the study area in South America in Grey. The map in the top right shows the main course of the Maroni basin, with the Maroni River constituting the border between Suriname and French-Guiana. The top left boxplots present the difference in cumulative precipitation between November 2017 and November 2021, with the mean cumulative precipitation represented by a black dot. These data are based on six meteorological stations located within the Maroni basin (Meteo France, data available online: https://meteo.data.gouv.fr/datasets/donnees-climatologiques-de-base-mensuelles).

sessions, water level was higher in 2021 than in 2017 (mean difference in precipitation (mm) ± se: 48.08 ± 24.14). The metadata associated with the samples are described in Table S1.

2.2. eDNA collection and processing

2.2.1. eDNA collection

We collected environmental DNA (eDNA) from water samples at 32 locations (hereafter, sites) along the main channel and the major tributaries of the Maroni in November 2017 and November 2021 to retrieve fish and mammal communities (Fig. 1). At each location, the river was wider than 20 m and deeper than 1 m (Strahler orders 5–7). The sites were sequentially sampled from downstream to upstream. Following the protocol of Cantera et al. (2019), we collected eDNA by filtering two replicates during 30 min and resulting approximately in 30 L of water per site. A peristaltic pump (Vampire Sampler; Buerkle GmbH, Bad Bellingen, Germany) and single-use tubing were used to pump the water into a single-use filtration capsule (VigiDNA, 0.45 μm; SPYGEN, Bourget-du-Lac, France). The tubing input was placed a few centimetres below the water surface in zones with high water flow as recommended by Cilleros et al. (2019). At the end of filtration, the capsule was drained, filled with 80 mL CL1 conservation buffer (SPYGEN), and stored in the dark before DNA extraction.

The collection of eDNA was adjusted to the environmental conditions in 2021. In 2021, water filtration and eDNA collection were conducted from a boat that navigated from one bank to the other to perform lateral transects, thereby maximising eDNA collection by sampling the entire width of the river. In 2017, the water level was too low to allow the boat to navigate between banks. Sampling was thus performed in turbulent areas to ensure optimal eDNA homogeneity throughout the water column.

2.2.2. eDNA laboratory and bioinformatics

For DNA extraction, each filtration capsule was agitated on an S50 shaker (Ingenieurbüro CAT M. Zipperer GmbH, Ballrechten-Dottingen, Germany) at 800 rpm for 15 min, decanted into a 50 mL tube, and centrifuged at 15,000 ×*g* and 6 °C for 15 min. The supernatant was removed with a sterile pipette, leaving 15 mL of liquid at the bottom of the tube. Subsequently, 33 mL of ethanol and 1.5 mL of 3 M sodium acetate were added to each 50 mL tube, and the mixtures were stored at −20 °C for at least one night. The tubes were then centrifuged at 15,000 ×*g* and 6 °C for 15 min, and the supernatants were discarded. Then, 720 μL of ATL buffer from a DNeasy Blood & Tissue Extraction Kit (Qiagen, Hilden, Germany) was added. The tubes were vortexed and the supernatants were transferred to 2 mL tubes containing 20 μL Proteinase K (Macherey-Nagel GmbH, Düren, Germany). The tubes were then incubated at 56 °C for 2 h. DNA extraction was performed using a NucleoSpin Soil kit (Macherey-Nagel GmbH, Düren, Germany) starting from step six of the manufacturer's instructions. Elution was performed by adding 100 μL of SE buffer twice. After the DNA extraction, the samples were tested for inhibition by qPCR following the protocol of Biggs et al. (2015). Quantitative PCRs were performed in duplicate for each sample. If at least one of the replicates showed a different Ct (Cycle threshold) than expected (at least 2 Cts), the sample was considered inhibited and diluted 5-fold before the amplification.

For fish, we used the TELEO marker (Valentini et al., 2016) (forward: 5′-ACACCGCCCGTCACTCT-3′; reverse: 5′-CTTCCGGTACACTTACCATG-3′), which has been shown to provide efficient discrimination of the local fish fauna (Cantera et al., 2019; Cilleros et al., 2019). For mammals, we used the 12S—V5 marker (Riaz et al., 2011) (F 5′-TAGAACAGGCTCCTCTAG-3′; R 5′-TTAGATACCCCACTATGC-3′) well suited to discriminate French Guianese mammals (Kocher et al., 2017). The DNA amplifications were performed in a final volume of 25 μL containing 1 U AmpliTaq Gold DNA Polymerase (Applied Biosystems, Foster City, CA, USA), 0.2 μM of each primer, 10 mM Tris-HCl, 50 mM KCl, 2.5 mM MgCl2, 0.2 mM of each dNTP, and 3 μL DNA template and 0.2 μg/μL bovine serum albumin (BSA; Roche Diagnostics, Basel, Switzerland). For fish amplification, the TELEO human blocking primer (Valentini et al., 2016) (5′-ACCCTCCTCAAGTATACTTCAAAGGAC-C3–3′) was added to the mixture and for mammal amplification, the following human blocking primer was added (5′-CTATGCTTAGCCCTAAACCTCAACAGTTAAATCAACAAAACTGCT-C3–3′, De Barba et al., 2014), both with final concentrations of 4 μM. Twelve PCR replicates were performed per field sample for each taxon (32 sites × 2 years × 2 field replicates x 12 PCR replicates x 2 taxa, 3072 PCR replicates in total). The forward and reverse primer tags were identical within each PCR replicate for TELEO marker and the forward and reverse primer tags were identical within each field sample for 12S—V5. The PCR mixture was denatured at 95 °C for 10 min, followed by 50 cycles of 30 s at 95 °C, 30 s at 55 °C for both markers and 1 min at 72 °C, and a final elongation step at 72 °C for 7 min. This step was conducted in a dedicated room for DNA amplification that is kept under negative air pressure. The success of the amplification was verified using capillary electrophoresis (QIAxcel; Qiagen GmbH) and the samples were purified using a MinElute PCR purification kit (Qiagen GmbH). Before sequencing, purified PCR products were quantified using capillary electrophoresis and then pooled in equal volumes to achieve an expected sequencing depth of 500,000 reads per sample before DNA library preparation.

Libraries preparation were performed at Fasteris facilities (Geneva, Switzerland) using a Metafast protocol (www.fasteris.com/metafast) for 2017 samples and at DNA Gensee (www.dnagensee.com) using the TruSeq kit (Illumina) following the manufacturer's instructions for 2021 samples. For the fish analyses, a total of 12 libraries were prepared, with six libraries for each year. For the vertebrate analyses, 13 libraries were prepared, consisting of seven libraries for the 2017 samples and six for the 2021 samples. Four libraries were sequenced on an Illumina HiSeq 2500 (2 × 125 bp) (Illumina, San Diego, CA, USA) with a HiSeq SBS Kit v4 (Illumina), three were sequenced on a MiSeq (2 × 125 bp) (Illumina) with a MiSeq Flow Cell Kit Version3 (Illumina), one library was sequenced on an Illumina HiSeq 2500 (2 × 125 bp) (Illumina, San Diego, CA, USA) with a HiSeq SBS Kit v4 (Illumina), the remaing libraries were sequenced on a NextSeq (2 × 150 bp + 8) (Illumina) with a NextSeq Mid kit (Illumina). Fourteen negative extraction controls and four negative PCR controls (ultrapure water, 12 replicates) were amplified per primer pair and sequenced in parallel to the samples to monitor possible contaminants. Sequencing was performed according to the manufacturer's instructions at Fasteris.

We analysed the sequence reads with the OBITools (Boyer et al., 2016) according to the protocol described by Valentini et al. (2016). Briefly, the forward and reverse reads were assembled with the `illuminapairedend` programme. We then used `ngsfilter` to assign the sequences to each sample. We created a separate dataset for each sample by splitting the original dataset into several files with `obisplit` and discarded sequences shorter than 20 bp or occurring <10 times per sample. We also discarded sequences labelled by the `obiclean` programme as “internal” and probably corresponding to PCR errors. We used the `ecotag` software for taxonomic assignment of molecular operational taxonomic units (MOTUs). For fish, we used an updated version of the reference database from Cilleros et al. (2019), incorporating an additional 183 species. The updated database now covers 364 (91 %) of the 400 freshwater fish species documented in French Guiana, with one to eight individuals per species sequenced (1600 sequences in total). 36 species (9 %) remain absent from the database due to the unavailability of DNA samples. We compared with the GenBank nucleotide database, but it contained limited information on fish species native to French Guiana. For mammals, we downloaded the EMBL-EBI vertebrate database from the European Nucleotide Archive (ENA) (http://ftp.ebi.ac.uk/pub/databases/embl/release/std/, release 142). We extracted the relevant metabarcoding fragment from this database using `ecopcr`. The resulting reference database included the local database of French Guianese mammals (Kocher et al., 2017), 576 specimens representing 164 species, along with all vertebrate species available in the

EMBL database. We evaluated species-level assignments only for ≥98 % sequence identity with the reference database and discarded sequences below this threshold. Given the incorrect assignment of a few sequences to the samples due to tag-jumps (Schnell et al., 2015), we also discarded all sequences with a frequency of occurrence <0.001 per sequence and per library. We curated the data obtained for Index-Hopping (MacConaill et al., 2018) with a threshold empirically determined for each sequencing batch using experimental blanks (*i.e.*, combinations of tags not present in the libraries). For the 2017 samples sequenced on a NextSeq platform, we discarded the species present in one to four lanes, based on the threshold empirically determined using experimental blanks. For the 2021 samples sequenced on a NextSeq platform, this filter was not necessary. These bioinformatic analyses provided species by site matrices for fish (Table S2a) and mammals (Table S3a) with presence/absence for each species.

2.3. Disturbance intensity

We quantified deforestation using the Global Forest Change database (Hansen et al., 2013). This dataset identifies areas deforested between 2001 and 2021 at a 30 m spatial scale. We considered deforestation intensity around each eDNA sampling site as an integrative measure of human-mediated environmental disturbances including gold mining, logging, agriculture, and human settlements (Cantera et al., 2022). We therefore refer to deforestation as an integrative measure of anthropogenic disturbances, where deforested areas can be associated with other disturbances, such as impacts on water quality caused by gold mining activities, or hunting and fishing near human settlements. We calculated the mean percentage of deforestation upstream of the sampling sites (along the sub-basin drainage network) within spatial extents of 30 km. Fig. S1 provides a schematic representation of the calculation of deforestation percentage for each site. We considered this spatial extent because we previously showed that 30 km represented the most relevant upstream spatial extent to investigate biodiversity responses to deforestation in our system (Cantera et al., 2022). We considered the sites' upstream sub-basin drainage network areas because it considers the hydrologic connectivity of rivers and the associated water-mediated downstream transfer of matters and pollutants. We delineated sub-basins by applying a Flow Accumulation algorithm to the SRTM Global 30 m Model Elevation (Becker et al., 2009). Then, for each sampling site, we quantified deforestation intensity by summing upstream deforested surfaces and dividing this sum by the area of the delineated spatial extent to obtain percentages of deforested surfaces.

2.4. Biodiversity measures

We generated fish and mammal site species inventories (presence/absence) from the collected eDNA. In this study system, both taxa groups were already shown to be reliably inventoried with eDNA metabarcoding (Cilleros et al., 2019; Coutant et al., 2021). Only the detections at species level were conserved and we removed the Chiroptera from the mammal inventories because our current reference database did not allow a reliable species discrimination of this group. We measured the taxonomic diversity of fish and mammal communities at the sites using species richness and we investigated the functional structure of fish and mammal communities using five functional indices computed with the framework of Mouillot et al. (2013).

2.4.1. Traits selection

We used morphological and ecological traits to functionally characterise fish and mammal communities. We used a local database for fish morphological traits, which includes 10 measurements of mature fish measured from side-view pictures, to compute 9 unitless ratios (hereafter referred to as traits) reflecting food acquisition and locomotion strategies (Villéger et al., 2017) (Table S2b & Table S4a). To compute this database, we measured morphological traits for as many individuals as possible and we used the averages of all measurements per species. For the ecological traits, we selected five qualitative traits related to trophy, behaviour and habitat preference collected from FishBase (http://www.fishbase.org) and the literature. For mammals, we compiled a total of 9 traits reflecting life strategies from different databases to maximise the number of traits and minimise the missing values (Table S4b & Table S3b). We selected the longevity, gestation length, litter or clutch size and adult body mass data from the Amniote database (Myhrvold et al., 2015) and the activity cycle, habitat and diet breadth, trophic level and terrestriality data from the Pantheria database (Jones et al., 2009). For continuous variables with varying numbers of measurements per species, trait values were represented by either the median or the mean, depending on the trait.

2.4.2. Building functional spaces

For fish, missing traits values represented 7.76 % of the trait dataset while it represented 9.94 % for mammals. We did not replace missing values as the two most used methods were not optimal in our case. The first method involves replacing missing trait values by randomly assigning values from the closest related species (Penone et al., 2014). We investigate small-scale temporal changes of communities that could result in small community structure changes. Changes may become undetectable when replacing missing trait values by the closest species as it can result in the homogenisation of the traits values. The second method involves machine learning approaches based on species phylogeny, which can be effective (Penone et al., 2014), but no reliable phylogenies were available to perform the inferency. Site functional space were computed based on the species trait values for both fish and mammals using the mFD package (Magneville, 2024) and the function *funct.dist* specifying the Gower distance that considers categorical and continuous traits while handling missing data and scale-centring trait values. We built functional spaces for fish and mammals separately, based on the global pool of species including all the species detected in 2017 and in 2021. The optimal number of PCoA axes maximising the quality of the functional spaces was selected using the *quality.fspaces* function that computes the square deviation between the scaled Euclidean distance and the Gower distance in the PCoA space using an increasing number of axes. The optimal number of PCoA axes minimises the square deviation between the scaled Euclidean and Gower distances, resulting in four and two axes for fish and mammals, respectively. For mammals, the number of axes was not the most optimal but we were constrained by the smallest site species richness as the sites must possess a higher number of species than PCoA axes. With two axes, the number of sites available to characterise the functional diversity of mammals drop to 28 sites out of the 32 sites sampled (M06, M08, M09, and M20 were excluded) while for fish the entire site dataset could be used. The fish coordinates onto the PCoA are provided in Table S2c and in Table S3c for mammals.

The *envifit* function in the vegan package of R was used to fit the variables (traits) onto the PCoA ordination and identify any correlations between the traits and the ordination axes. We computed the determination coefficients r^2 to assess the strengths of the correlations between the axes and the traits. *P*-values were computed by comparing the observed and simulated r^2 based on 999 random data permutations. To quantify the trait contributions, we transformed the continuous variables onto vectors directed according to their correlation with the axes. Their lengths were proportional to the strengths of the correlations between the ordinations and the traits (r^2) (Table S5a). For the categorical variables, we computed the average ordination scores from the scores of all species belonging to each factor level to locate categories in the functional spaces (Table S5b).

2.4.3. Functional indices

The functional facets of fish and mammal communities at the sites were characterised by the functional indices of Villéger et al. (2008) using the function *alpha.fd.multidim*. Five functional indices were

computed (FDis, FDiv, FEve, FOri and FRic) resulting in observed functional indice values for each taxon, each site and each year (Table S1). With presence/absence data and not abundance, these indices ranging from 0 to 1 can be interpreted as follow. The functional dispersion (FDis) reflects the deviation of the species trait values from the centre of the functional space filled by the community and therefore, the species functional distance to the mean trait values of the community. The functional divergence (FDiv) assesses the level of functional difference between species in the functional space. Lower values reflect species close to the assemblage centroid in the occupied volume while higher values highlight species that are distant from the assemblage centroid. High FDiv values reflect high levels of niche differentiation and therefore low interspecific competition. The functional evenness (FEve) is the regularity of the distribution of species in the functional space, which allows estimating if species are concentrated or dispersed evenly in the functional space. The functional originality (FOri) represents the functional isolation of species in the functional space and is calculated by computing the functional distance between all species pairs. The functional richness (FRic) is the convex hull volume occupied by co-occurring species at each site in the functional space. Higher values reflect high volume occupation and, therefore, high functional diversity (Freitas et al., 2021; Mouillot et al., 2013; Villéger et al., 2017).

2.4.4. SES Functional indices

The diversity of functions in assemblages is generally correlated with the number of species. To disentangle functional diversity from species richness gradients, we used null models and standardised effect size (SES) to distinguish between the effect of species number and underlying processes influencing functional patterns (Gotelli, 2000; Swenson, 2014). We built null models for each taxon (fish and mammals) using global species pools including all the species detected in 2017 and 2021. From these global species pools, we built species pools per Strahler order as this indice correlates with the position in the upstream-downstream gradient and indicates different habitats and river sizes. We computed null models by generating simulated communities composed of species randomly drawn from the Strahler order species pools. The simulated communities were constrained to conserve the observed site species richness and species observation frequencies using the function *randomizeMatrix* function from package Picante (Kembel et al., 2020) and the "Independent Swap" algorithm (Gotelli, 2000). 1000 communities were simulated for each sites (32 sites in total) and sample year (2017 and 2021) to compute null distributions for the five functional indices. Then, we calculated the standardised effect size (SES) corresponding to the difference between the observed functional indices and the mean of the 1000 simulated values of functional indices divided by the standard deviation of these 1000 null values. Therefore, the functional SES indices constitute functional measures that are independent from taxonomic diversity (Swenson, 2014). SES values for each functional indices and for both taxa are provided in Table S1.

2.5. Data analyses

Given the methodological adjustments in eDNA sampling (static *versus* lateral transects, detailed in the *eDNA collection* section) and variations in water levels between the two years, direct temporal comparisons of species richness and functional indices dependent on species richness could result in biased interpretations. Within each year, spatial comparisons between sites along the longitudinal upstream-downstream gradient remain valid, as eDNA collection was conducted using consistent protocols and under similar environmental conditions. We compared the distance decay of species similarity between 2017 and 2021 to assess whether changes in the environment and eDNA sampling method influenced community ß-diversity along the longitudinal gradient. We observed that fish and mammal communities exhibited the same patterns of differentiation along the watercourse in both years (Fig. S2), which suggests that the differences in environmental conditions and eDNA sampling between 2017 and 2021 did not influence the ß-diversity patterns along the Maroni River.

2.5.1. Taxonomic and functional models

Using Generalised Linear Mixed Models (GLMMs), we investigated biodiversity changes along the upstream-downstream gradient within each year in relation to deforestation. Since deforestation was used as a proxy for anthropogenic disturbances, the biodiversity response we measured reflected not only the direct effects of deforestation but also the broader impacts of the disturbances driving deforestation. For the taxonomic facet, we built four models (two years x two taxa) using the *glmmTMB* package (Brooks et al., 2017) with a Poisson distribution for the species richness count variable. We assessed residual spatial autocorrelation using Moran's I tests. Models exhibiting significant spatial autocorrelation were adjusted by specifying a correlation structure for the residuals based on site coordinates. We tested the three spatial correlation structures implemented in the glmmTMB package: Gaussian, Matérn, and exponential. The best model was then selected based on the Akaike information criterion (AIC). The significance of the effect of each deforestation was tested using the Wald test with a critical significance level of 0.05. Model assumptions were then evaluated using the *performance* (Lüdecke et al., 2019) and *DHARMa* (Hartig and Lohse, 2022) packages.

We investigated functional changes along the upstream-downstream gradient within each year in relation to deforestation using Generalised Least Squares (GLS) models, implemented in the *nlme* package (Pinheiro et al., 1999). GLS are more flexible than Ordinary Least Squares (OLS) models, allowing for the accommodation of correlation or heteroscedasticity in the residuals when modeling Gaussian data. Twenty models (two taxa × five functional indices × two years) were built, and residual spatial autocorrelation and heteroscedasticity were tested for each model using Moran's I tests and Breusch-Pagan tests, respectively. Models presenting spatial autocorrelation in the residuals were adjusted by specifying a correlation structure based on site coordinates. We tested models with different spatial structure (spherical, Gaussian, circular, linear and exponential) and selected the best fitting model using AIC. Models with residual heteroscedasticity were adjusted by specifying a residual variance structure based on the site's distance to the estuary. We tested three variance structures: the exponential variance function structure, the power variance function structure, and the constant-plus-power variance function structure. We selected the best-fitting model using AIC. To assess the significance of deforestation, we tested the estimated regression coefficients using *t*-tests, evaluating whether each coefficient significantly differed from zero. We verified model assumptions using the performance and DHARMa R packages. Models with and without residual correlation structures and variance structures are presented in Table S6 for taxonomic models and in Table S7 and Table S8 for functional models.

2.5.2. Comparing deforested and non-deforested sites

To identify whether the functional spatial trends of communities were solely driven by changes in species richness or reflected underlying ecological processes influencing functional diversity, we assessed whether the mean SES functional indice values in deforested and non-deforested sites were significantly different from zero. If the mean was significantly different from zero, we assumed that indices deviated from the null expectation and that functional patterns were not only the reflect of species richness. Sites were classified by deforestation level into deforested sites (deforested area exceeding 0.33 %) and non-deforested sites (deforested area < 0.33 %, explained by natural forest turnover or tree falls). This threshold was determined by measuring natural deforestation at 100 randomly selected sites in areas without human settlement, human activity, or anthropogenic deforestation. For the taxonomic facets, we statistically compared species richness between deforested and non-deforested sites within both years using unpaired two-samples t-tests when data followed a normal distribution and

unpaired two-samples Mann-Whitney *U* tests when data deviated from the normal distribution. For the functional facet, we used One-sample t-tests to estimate whether the means of the SES functional indice values in deforested as well as in non-deforested sites were significantly different from zero. We did not perform direct comparisons of species richness between the two years because of the background variability introduced by eDNA sampling adjustment and environmental variability.

2.5.3. Temporal comparison of longitudinal species distribution

We assessed whether the communities displayed distinct spatial trends along the river between 2017 and 2021 by evaluating the effect of the sampling year on the slopes of the taxonomic and functional models. This analysis was performed with an Analysis of Covariance (ANCOVA). For both functional and taxonomic facets, fixed effects were modeled as the interaction between deforestation and sampling year. Both variables were scaled and centered to mitigate convergence issues. The associated *p*-values, estimated using Wald tests for taxonomic glmmTMB models and t-tests for GLS functional models, indicate whether the model slopes differ significantly between 2017 and 2021. Detailed ANCOVA results are provided in **Table S9.**

3. Results

3.1. General results

During the two sampling campaigns, a total of 185 fish species were detected. In 2017, 176 species were detected, with species richness per site ranging from 7 to 132 (median = 62.5, sd = 35.35). In 2021, 184 fish species were detected resulting in a species richness per site ranging from 24 to 135 (median = 80.5, sd = 34.64). For mammals, 54 species were detected, with 41 species detected in 2017 and all the 54 species detected in 2021. In 2017, species richness per site varied from 1 to 20 (median = 7, sd = 4.68), while it ranged from 4 to 32 (median = 8, sd = 8.35) in 2021.

The deforestation of the Maroni basin represented 472.38 km^2 in 2017 (0.70 % of the Maroni basin) and 658.90 km^2 in 2021 (0.97 % of the Maroni basin). 186.52 km^2 were therefore deforested between 2017 and 2021 representing an increase of 0.27 %. The period 2017–2021 was therefore characterised by a mean annual deforestation rate of 46.63 km^2 or 0.07 % compared to the mean annual deforestation rate of 34.64 km^2 (0.05 %) recorded for the period 2000–2023. The sites' deforestation percentages and hectares (considered over an area extending from each site to 30 km upstream) significantly increased between 2017 and 2021 (Paired Mann-Whitney U tests test, $p < 0.001$***) (Fig. 2a, b). Increased deforestation occured at most of the sites except for six sites (M15, M28, M29, M30, M31 and M32) (Fig. 2a, b), all located upstream from Pidima village apart from M15. In 2017, the site deforestation ranged from 0 % (0.51 ha) to 5.90 % (4472.80 ha) with a mean deforestation of 1.59 % (1150.15 ha) (median = 0.74 % and 460.97 ha, sd = 1.9 3 % and 1486.70 ha). In 2021, the site deforestation ranged from 0 % (0.51 ha) to 8.20 % (6441.93 ha) with a mean deforestation of 2.13 % (1595.37 ha) (median = 1.04 % and 612.62 ha, sd = 2.55 % and 2024.74 ha) (Fig. 2a, b).

3.2. Spatiotemporal taxonomic changes in 2017 and 2021

Species richness of fish significantly decreased with increasing deforestation percentages in both 2017 and 2021 (Fig. 3a; Table 1). In 2017, species richness in non-deforested sites was 2.19 times higher than in deforested sites ($t_{(20.8)} = -6.45$, $p < 0.001$***), while it was 1.88 higher in 2021 ($t_{(27.7)} = -7.40$, $p < 0.001$***). The ANCOVA analysis revealed a significant effect of the year on the models' slopes ($F_{(1)} = 7.91$, $p < 0.01$**) with a smaller slope in 2021 (slope = −0.16) compared to 2017 (slope = −0.15, Fig. 3a; Table 1; Table S9).

Similarly for mammals, species richness decreased with increasing deforestation percentages in both 2017 and 2021 (Fig. 3b; Table 1). In 2017, species richness in non-deforested sites was 1.6 times higher than in deforested sites (W = 67.5, $p < 0.05$*), while it was 2.22 times higher in 2021 (W = 21, $p < 0.001$***). The ANCOVA analysis did not evidence any significant effect of the year on the models' slopes (Table S9).

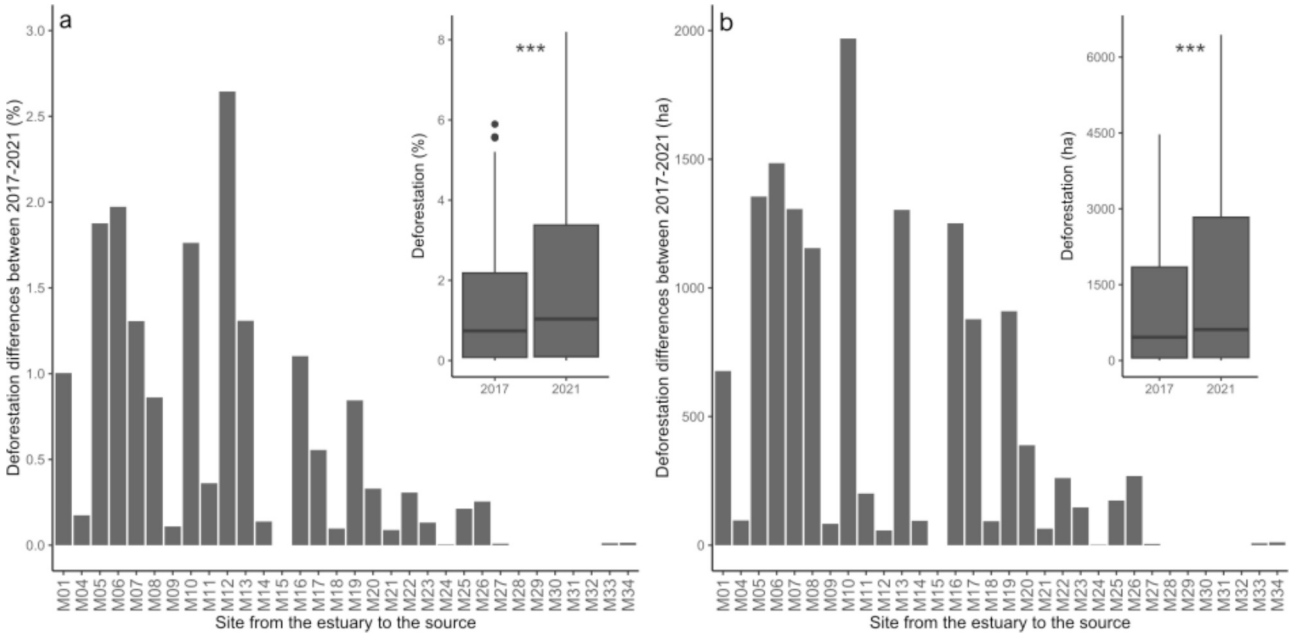

Fig. 2. Upstream deforestation increase between 2017 and 2021 in percentage (a) and in hectares (b) at each sites. The boxplots show the mean deforestation percentage (a) and hectares (b) for 2017 and 2021. Deforestation was assessed over a 30 km upstream sub-basin drainage area for each site as Cantera et al. (2022) demonstrated that this is the most relevant spatial extent at which considering deforestation impacts on biodiversity (see Fig. S1). Sites are ordered from the estuary to the source. The percentages and hectares of deforestation can result in different site ranking because the area and the shape of each upstream sub-basin drainage network vary with the shape of the river. The difference in deforestation percentage and hectares was compared using a Paired Mann-Whitney *U* tests, $p < 0.001$***.

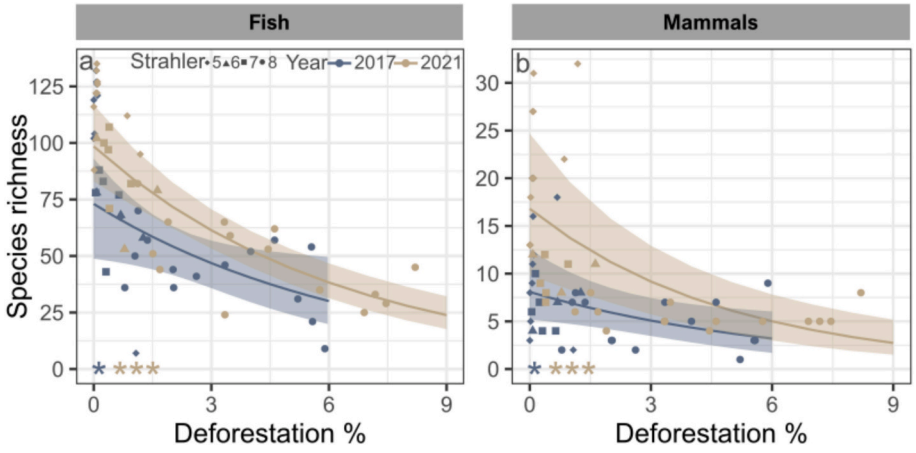

Fig. 3. Effects of deforestation on fish (a) and mammal (b) species richness in 2017 and in 2021. Solid lines represent the fitted values of glmmTMB Poisson models, with light shading indicating 95 % confidence intervals. Residual spatial autocorrelation was assessed using Moran's I tests, and models were adjusted with a residual correlation structure when necessary. The optimal residual structure was determined based on AIC values. Model significance, determined using Wald tests, is indicated in the bottom-left corner of each panel: ns = not significant, $p < 0.05$*, $p < 0.01$**, $p < 0.001$***. A total of 32 sites were sampled in both 2017 and 2021. Detailed model estimates, significance, AIC values, and test *p*-values are provided in **Table S6**.

Table 1
Results of the taxonomic and functional models relating species richness and SES functional indices to the percentage of upstream deforested surfaces in 2017 and 2021 for both fish and mammals.

Taxa	Year	SR	FDis	FDiv	FEve	FOri	FRic
Fish	2017	−0.148 *	0.295 ns	−0.966 *	0.406 *	0.796 **	−0.269 *
	2021	−0.158 ***	−0.177 ns	−0.364 ns	0.32 ***	0.551 **	−0.301 **
Mammals	2017	−0.154 *	−0.375 ns	0.395 ns	−1.36 **	−0.086 ns	−0.435 **
	2021	−0.202 ***	−0.031 ns	0.171 ns	−0.349 ns	−0.206 ns	−0.118 ns

Each cell includes the slope estimates and model significance: ns = not significant, $p < 0.05$*, $p < 0.01$**, $p < 0.001$***. When necessary, models were adjusted with residual correlation or variance structures to account for spatial autocorrelation and heteroscedasticity. The optimal residual structure was selected based on AIC values. Detailed model estimates, significance, AIC values, and test p-values are provided in **Tables S6; S7** and **S8.** SR refers to species richness.

3.3. Spatiotemporal functional changes in 2017 and 2021

For fish communities, the SES values of functional dispersion (FDis) did not significantly differ from zero and were not associated with deforestation in 2017 nor in 2021 (Fig. Fig. 4a, b; Table 1). By contrast, the SES values of functional divergence (FDiv) significantly decreased with increasing deforestation percentages in 2017 (Fig. Fig. 4d; Table 1), but the association between functional divergence and deforestation was solely supported by species richness as the SES values did not significantly differ from zero in the deforested sites (Fig. Fig. 4c). We found a contrasting trend for the SES values of functional evenness (FEve), which significantly increased with increasing deforestation percentages in 2017 and in 2021 (Fig. Fig. 4f; Table 1). In 2017, the association between functional evenness and deforestation was independent of species richness (deforested: $t_{(18)} = 3.11$, $p < 0.01$**, non-deforested: $t_{(12)} = -10.61$, $p < 0.001$***), while in 2021, SES values did not significantly differ from zero (Fig. Fig. 4e). Similarly, the SES values of functional originality (FOri) significantly increased with increasing deforestation percentages in 2017 and in 2021 (Fig. Fig. 4 h; Table 1) but only the non-deforested sites of 2017 and 2021 exhibited functional originality patterns not only supported by species richness (2017: $t_{(12)} = -7.85$, $p < 0.001$***, 2021: $t_{(9)} = -6.61$, $p < 0.001$***; Fig. Fig. 4 g). The SES values of functional richness (FRic) significantly decreased with increasing deforestation percentages in both 2017 and 2021 (Fig. Fig. 4j; Table 1). The SES values of both non-deforested and deforested sites were all significantly different from zero, indicating that functional richness patterns were not solely supported by species richness at these sites (2017 non-deforested: $t_{(12)} = 5.38$, $p = 0 < 0.001$***, 2017 deforested: $t_{(18)} = -4.32$, $p < 0.001$***, 2021 non-deforested: $t_{(9)} = 4.93$, $p = 0 < 0.001$***, 2021 deforested: $t_{(21)} = -2.76$, $p < 0.05$*; Fig. Fig. 4i).

The ANCOVA analysis indicated no significant influence of the year on the functional SES regression models' slopes (Table S9).

For mammal communities, most models did not show a significant relationship between deforestation and functional SES indices, with only two significant models observed. The SES values of functional evenness significantly decreased with increasing deforestation percentages in 2017 (Fig. 5f; Table 1), but the SES values were not significantly different from zero (Fig. 5e). Similarly, the SES values of functional richness in 2017 significantly decreased with increasing deforestation percentages (Fig. 5j; Table 1). In this year, the SES values of deforested sites were not only supported by species richness ($t_{(14)} = -3.01$, $p < 0.01$**).

The ANCOVA analysis did not evidence any significant influence of the year on the SES regression models' slopes except for functional evenness (ANCOVA, $p < 0.01$**; Table S9).

4. Discussion

Understanding the driving processes and associated community patterns at both spatial and temporal scales is pivotal to assess and predict the fate of biodiversity in the Anthropocene (Gonzalez et al., 2016; Su et al., 2021). Elucidating the mechanisms underlying observed patterns requires a comprehensive and dynamic view of organisms' distribution through time and space (Gonzalez et al., 2016). While recent advances in the field of eDNA are improving our understanding of species distribution and the underlying processes, the routine application of these methods for temporal biodiversity monitoring remains challenging. Standardised protocols are required, while our understanding of eDNA ecology and protocol optimisation is still in progress

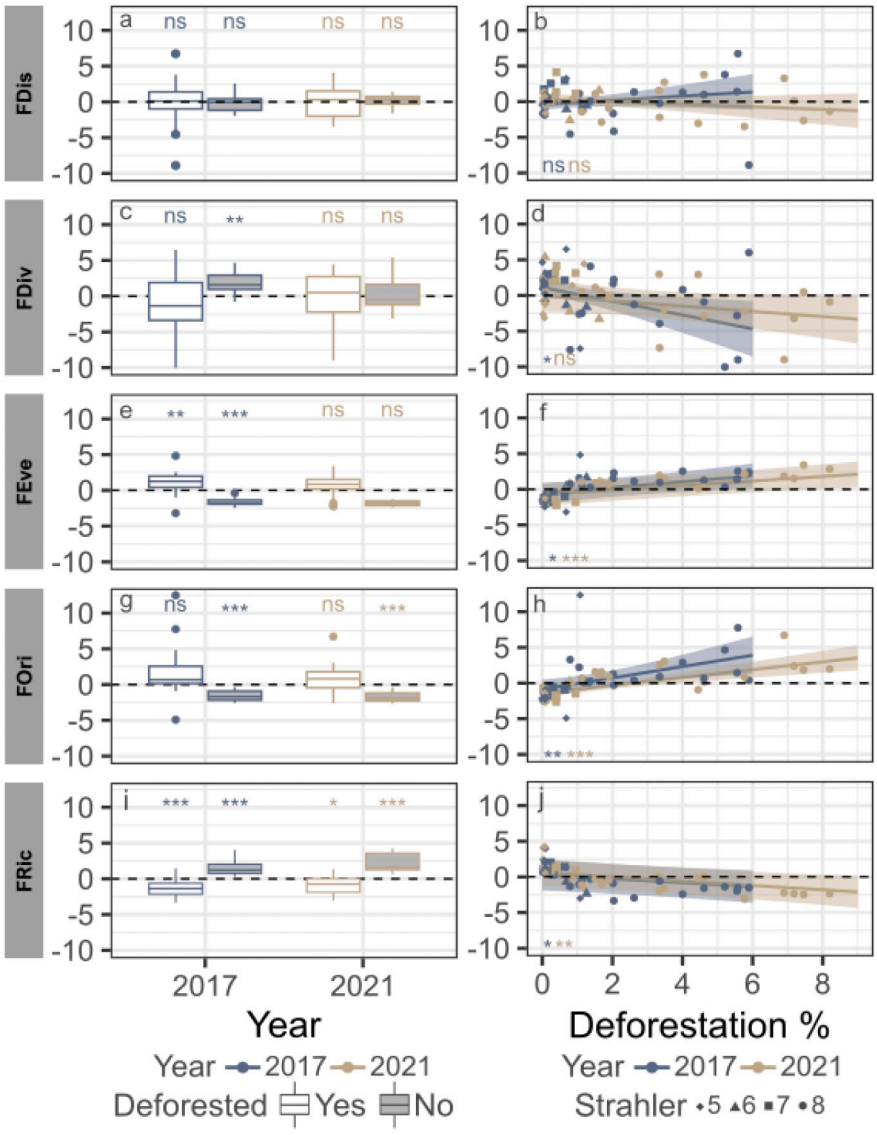

Fig. 4. Effects of deforestation on SES functional indices for fish in 2017 and 2021. Panels a, c, e, g, and i show deviations of deforested and non-deforested SES functional indice values from random expectation, with one-sample *t*-tests determining whether SES mean values significantly differ from zero. Panels b, d, f, h, and j presents the GLS models relating SES functional indices to deforestation percentages. Solid lines indicate model-fitted values, with light-colored shading representing 95 % confidence intervals. Residual spatial autocorrelation was assessed using Moran's I tests, and heteroscedasticity was examined using Breusch-Pagan tests. When necessary, models were adjusted with residual correlation or variance structures to account for spatial autocorrelation and heteroscedasticity. The optimal residual structure was selected based on AIC values. Model significance for each year is noted in the bottom-left corner of each panel: ns = not significant, $p < 0.05$*, $p < 0.01$**, $p < 0.001$***. Detailed model estimates, significance, AIC values, and test p-values are provided in **Tables S7** and **S8.**

(Blackman et al., 2024; Mathieu et al., 2020; Schenekar, 2023). Here, we investigated spatiotemporal changes in fish and mammal communities along the longitudinal upstream-downstream gradient of the Maroni River between 2017 and 2021 using eDNA. During this short time frame, our study area experienced a slight increase in deforestation (+0.27 %) mainly localised in the downstream section of the river. In this context, we question whether eDNA provides sufficiently fine-scale data to detect associated biodiversity changes, despite environmental effects and protocol adjustments introducing background variability in the data.

4.1. Longitudinal trends in fish and mammal diversity over four years

The biodiversity declines associated with deforestation levels along the longitudinal gradient, as previously observed Cantera et al. (2022), persisted in 2021. Declines were particularly observed at the most downstream sites —M1, M6, M5, and M12 for fish, and M1, M5, and M12 for mammals— which exhibited increased levels of deforestation. For fish communities, the monitoring year had a significant effect on the spatial species richness trends observed, with the longitudinal decline in 2021 being 1.07 times larger than in 2017. This indicates an increased impact of anthropogenic disturbances on fish species richness. In contrast, mammal communities showed no significant differences in the longitudinal trends of species richness decline between 2017 and 2021. Mammal diversity continued to decline at a consistent rate, with no significant changes in the pace of decline observed between years.

The increase in deforestation between 2017 and 2021 was also associated with continuous declines in functional richness for fish, but without significant changes in the rate of decline. This paired decline in species and functional richness suggests that extreme functional strategies, located at the boundaries of the functional space, are being impacted. As supported by the deviation of SES values from the null distribution, this loss of extreme functional strategies is not solely the result of random species loss but is also likely the result of ecological processes such as environmental filtering induced by anthropogenic

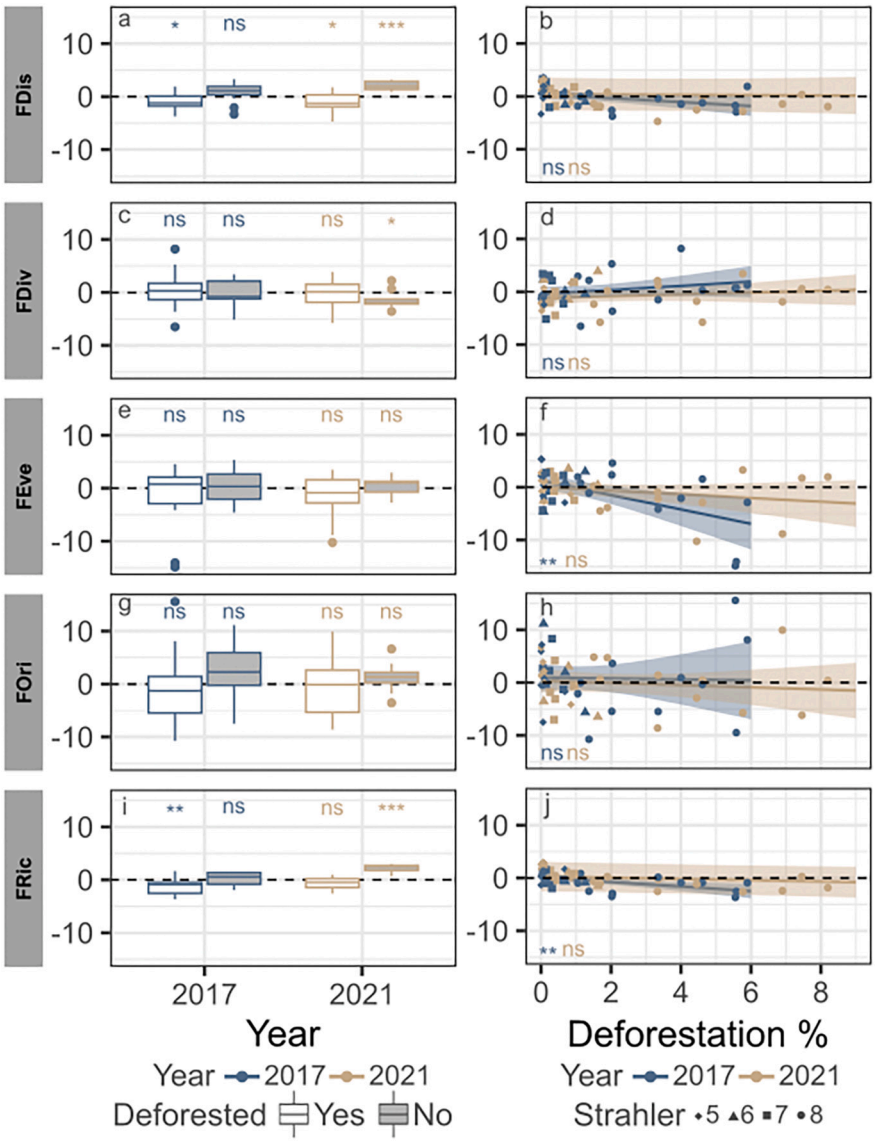

Fig. 5. Effects of deforestation on SES functional indices for mammals in 2017 and 2021. Panels a, c, e, g, and i show deviations of deforested and non-deforested SES functional indice values from random expectation, with one-sample t-tests determining whether SES mean values significantly differ from zero. Panels b, d, f, h, and j presents the GLS models relating SES functional indices to deforestation percentages. Solid lines indicate model-fitted values, with light-colored shading representing 95 % confidence intervals. Residual spatial autocorrelation was assessed using Moran's I tests, and heteroscedasticity was examined using Breusch-Pagan tests. When necessary, models were adjusted with residual correlation or variance structures to account for spatial autocorrelation and heteroscedasticity. The optimal residual structure was selected based on AIC values. Model significance for each year is noted in the bottom-left corner of each panel: ns = not significant, $p < 0.05$*, $p < 0.01$**, $p < 0.001$***. Detailed model estimates, significance, AIC values, and test p-values are provided in **Tables S7** and **S8**.

impacts (Cantera et al., 2023b, 2023a). These findings align with the global trends of functional richness losses in freshwater fishes (Carmona et al., 2021; Su et al., 2021). In contrast, the longitudial decline in mammals species richness was not significantly associated with deforestation in 2021.

Between the two monitored years and for both taxa, there was no evidence that an increase in the intensity of anthropogenic disturbances caused a shift in the functional structure of assemblages, but we observed a continuation of some changes at the same pace as observed in 2017. Fish communities exhibited a continuous loss of functional redundancy for generalist functions, as evidenced by the paired increase in functional evenness and originality, particularly observed in M01, M04, M05 and M06 downstream sites. Compared to fish communities, mammal communities did not exhibit consistent significant longitudinal trends in 2021.

4.2. *Longitudinal changes of fish and mammal assemblages*

For fish communities, the longitudinal increase in functional evenness and originality along the deforestation gradient contrasts with the more commonly observed patterns of decreasing functional evenness and originality as disturbance intensity increases in streams and rivers (Alvarenga et al., 2021; Cantera et al., 2023b; Leitão et al., 2018). For instance, in streams (Leitão et al., 2018) and rivers Cantera et al. (2023b), researchers observed a decline in functional evenness related to negative impacts on species with traits associated with the benthic compartment. They related this biodiversity response to deforestation, along with other anthropogenic activities such as gold mining, which significantly affect the benthic compartment and microhabitats by increasing water turbidity and siltation (Cantera et al., 2023b; Leitão et al., 2018; Silva et al., 2022; Teichert et al., 2018). In the Maroni River, the functional erosion of fish functional richness, combined with the

observed decline in functional redundancy of generalist functions may indicate a progressive reduction of functional insurance (*i.e* resilience) of the sites (Brejão et al., 2018). For mammals, longitudinal changes in the functional space with increasing deforestation were only significant in 2017, when mammal communities exhibited a decline in functional evenness along the longitudinal gradient. This pattern, associated with increasing deforestation percentages may indicates a reduction in the diversity of functional strategies within the functional space, but the lack of deviation of SES values to the random expectation suggests that these changes only reflected taxonomic modifications. Coupled to the longitudinal loss of functional richness with increasing deforestation, the decline in functional evenness indicates the loss of extreme functions located at the boundaries of the functional spaces (Carmona et al., 2021; Mouillot et al., 2013; Ripple et al., 2017). The reported trends are consistent with global and continental functional declines of species with extreme functional strategies, such as small and highly specialised vertebrates that are threatened by habitat loss and modification (Ripple et al., 2017).

Both fish and mammal communities showed evidence of declines in extreme functional strategies along the anthropogenic gradient. The pattern align with the globally observed trend of functional homogenisation, where specialist species are increasingly replaced by generalist species as a response to the loss of habitat diversity driven by anthropisation (Carmona et al., 2021). However, compared to fish communities, mammal communities showed no evident signs of decline in functional redundancy of generalist functions. This may be due to the lack of direct consideration of other major drivers of mammal diversity loss, such as hunting. Biodiversity assessments indicate that large, slow-paced species, like many large mammals, face higher extinction risks associated with hunting activities (Ripple et al., 2017). Despite the ongoing increase in anthropogenic disturbances, the Maroni River is part of one of the largest remaining wilderness areas in Amazonia, characterised by low historical deforestation rates (Dezécache et al., 2017; Watson et al., 2018). Ecological communities in these largely intact landscapes tend to harbor a higher number of species with narrow niches, making them disproportionately sensitive to ecosystem impacts (Watson et al., 2016). Therefore, the biodiversity of the Maroni region requires real-time monitoring, as it may exhibit intermediate, nonlinear and unpredictable taxonomic and functional changes in response to disturbances (Brejão et al., 2018; Chen and Olden, 2020). For instance, Brejão et al. (2018) evidenced a negative threshold response of stream fish to low deforestation levels (<20 %) and <5 years after the impacts. This negative threshold response was related to the decline of functionally unique sensitive species associated with complex habitat structures. In the present study, the spatiotemporal increase in functional evenness and originality in fish communities, which accompanies the decrease in the functional redundancy of some generalist functions, may reverse into a decrease in functional evenness when these generalist functions are only supported by a few species (Cantera et al., 2023b; Teichert et al., 2018).

4.3. Study limitation

Real-time spatiotemporal assessments of biodiversity are crucial for understanding and addressing biodiversity decline in environments continuously modified by anthropogenic activities. eDNA is widely recognised as a cost-effective tool for biodiversity monitoring, delivering rapid, multi-taxa assessments comparable in effectiveness to traditional methods such as netting, electrofishing, or transect surveys, which are typically labor-intensive (Keck et al., 2022). The signal from eDNA is particularly sensitive to environmental factors, such as water regimes and physicochemical conditions, which can influence its spatial and temporal distribution (Altermatt et al., 2023; Stewart, 2019). For example, higher river discharge rates may increase the longitudinal transport of eDNA while simultaneously increasing the dilution effect on eDNA concentrations (Van Driessche et al., 2023). Additionally, the eDNA decay rate may vary with water regimes, as it is influenced by factors such as water temperature, turbidity, acidity, UV exposure, and microbial activity (Harrison et al., 2019; Pont, 2024). The two years sampled in our study experienced varying levels of precipitation, but the distance decay of species similarity along the upstream-downstream gradient showed no significant differences between 2017 and 2021. This suggests that variations in precipitation levels and, consequently, water regimes, along with the adjusted sampling methodologies, were not sufficient to affect the ß-diversity of assemblages based on occurrence data. This may be due to the weak difference in intra-seasonal precipitation compared to inter-seasonal precipitation. The sampling campaigns conducted in November 2017 and 2021 showed a difference in precipitation levels of 48.08 mm ± 24.14 (mean ± SE), whereas inter-seasonal differences were significantly greater, with mean differences of 224.84 ± 29.49 mm in 2017 and 148.48 ± 29.40 mm in 2021 (Météo France data). From the perspective of implementing real-time temporal monitoring of biodiversity, these results should be compared across different levels of environmental variability to better identify the thresholds at which changes in precipitation and water regimes critically affect ß-diversity, and thus, spatial comparisons of communities.

Environmental variability did not significantly influence community differences along the longitudinal gradient but may have impacted species richness at individual sites and functional metrics dependent on species richness. As a result, we focused the analyses to spatial comparisons of species distributions, rather than direct temporal change in species numer or functional metric. The bias may be even more pronounced for non-aquatic organisms. eDNA methods often yield higher rates of false negatives in mammal surveys compared to fish surveys, as eDNA from mammals is less abundant in the water (Coutant et al., 2021; Lyet et al., 2021; Sales et al., 2020). Furthermore, detection rates may also be influenced by water regimes, as precipitation and rising water levels enhance the transfer of eDNA into aquatic systems through the inundation of riparian surfaces and water runoff (Lyet et al., 2021). This may explain the lack of continuous significant spatial trends in mammal communities between 2017 and 2021, despite increasing deforestation levels. The sensitivity of eDNA to environmental conditions challenges the use of eDNA for temporal biodiversity monitoring, as variability in these conditions can change unpredictably between monitoring periods. This hinders the ability to obtain reliable temporal estimates of biodiversity declines in response to anthropogenic impacts.

While coarse-scale data, such as species occurrences, can provide valuable information on community assembly, fine-scale data, such as abundance information, are necessary for a more precise understanding of community modifications. This is because certain processes of community modification may not be reflected in species presence/absence or may only become evident at critical stages, such as local extirpations of species. Species abundances, therefore, offer a more accurate representation of real-time community modifications. The functional structures of the Maroni fish and mammal communities may have exhibited different patterns with abundance data. Since generalist species are more abundant than specialists, abundance data could have evidenced a stronger impact of anthropogenic disturbances on functional metrics, emphasising the loss of extreme functional strategies. This is because abundance weighting shifts trait distributions toward generalist species, whereas occurrence data treats all species equally. Consequently, the contraction of functional space may have been more pronounced, highlighting a stronger process of functional homogenisation. However, it remains debatable whether eDNA methods can provide absolute estimates of species abundances at the community level, due to the numerous biotic and abiotic factors that make the relationship between eDNA concentration and species abundance inherently complex (Yao et al., 2022). Nonetheless, several studies, particularly in fish communities, have demonstrated the effectiveness of eDNA in reflecting relative species abundances within communities (Rourke et al., 2021). Current research on quantifying eDNA and developing models to account for its decay and transport under varying hydrological regimes

and environmental conditions will be crucial for advancing real-time biodiversity monitoring (Luo et al., 2023; Pont, 2024; Yao et al., 2022).

Given the study results and limitations, aquatic eDNA successfully detected changes in fish diversity in the context of small increase in anthropogenic disturbances, despite background variability introduced by environmental factors and protocol adjustments. For mammal communities, while eDNA provided insightful trends, a better understanding of the eDNA dynamics between terrestrial and aquatic landscapes is crucial to reflect biodiversity changes consistently (Newton et al., 2025).

5. Conclusion

Real-time biodiversity monitoring are pivotal to understand and monitor the progressive taxonomic and functional changes of biodiversity associated to the increase of anthropogenic pressure. Using spatially and temporally well resolved data, it is possible to compare the spatial changes of biodiversity within each period and associate it with subtle environmental changes. Such early identification of erosion can allow to tackle the problem before ecosystem has been too largely degraded. Over a four-year period characterised by a slight increase in anthropogenic disturbances, we observed a continuation of taxonomic and functional richness alteration downstream the Maroni River, without drastic changes in the intensity of the declines. Both fish and mammal communities showed evidence of declines in extreme functional strategies along the anthropogenic gradient but fish communities also exhibited a loss of functional redundancy in generalist functions. Given the continuous increase in anthropogenic activites along the Maroni River, these communities should be monitored over longer periods with short intervals to document the real-time reorganisation of their functional structure, which may not follow a linear trajectory and may undergo intermediate states.

Supplementary data to this article can be found online at https://doi.org/10.1016/j.scitotenv.2025.179021.

Author contribution

O.C., M. L.L., V.P., L.P., and S.B. conceived the ideas and designed methodology; S.B., M. L.L., J.B.D., V.P., and G.Q. collected the data; A.V. supervised the laboratory work and conducted the bioinformatic analyses; O.C. analysed the data; O.C., M. L.L., V.P., J.M., G.Q., L.P., S.B. led the writing of the manuscript. All authors contributed critically to the manuscript.

Conflicts of interest

Teleo primers and the use of the amplified fragment for identifying fish species from environmental samples are patented by the CNRS and the Université Grenoble Alpes. This patent only restricts commercial applications and has no implications for the use of this method by academic researchers. SPYGEN owns a license for this patent. AV and VP are research scientists at a private company specialising in the use of eDNA for species detection (SPYGEN).

CRediT authorship contribution statement

Opale Coutant: Writing – review & editing, Writing – original draft, Methodology, Investigation, Formal analysis, Data curation, Conceptualization. **Manuel Lopes-Lima:** Writing – review & editing, Validation. **Jérôme Murienne:** Writing – review & editing, Writing – original draft, Validation. **Loic Pellissier:** Conceptualization, Funding acquisition, Writing – review & editing. **Grégory Quartarollo:** Writing – review & editing, Resources. **Alice Valentini:** Writing – review & editing, Validation, Data curation. **Vincent Prié:** Writing – review & editing, Writing – original draft, Resources, Investigation, Funding acquisition, Conceptualization. **Sébastien Brosse:** Writing – review & editing, Writing – original draft, Validation, Supervision, Project administration, Methodology, Investigation, Funding acquisition, Conceptualization.

Acknowledgements

This work is part of the Vigilife Sentinel Rivers projects. It was supported by the Office de l'Eau Guyane, SPYGEN and Beauval Nature. OC, JM, SB benefited from Investissement d'Avenir grants managed by the Agence Nationale de la Recherche (CEBA: ANR-10-LABX-25-01; TULIP: ANR-10-LABX-0041)), We are indebted to the Guiana National Park (PAG), for authorizing access to the Guiana National Park core area and to R. Russo, M. Rhoné and J.B. Decotte for fieldwork support. We also thank SPYGEN staff for the laboratory technical support.

Data availability

Supplementary materials including Fig. S1 to S2 and Table S1 to S10 underlying the main results of the study are provided in the online version of the article. All Illumina raw sequences are available on figshare repository under accession code https://doi.org/10.6084/m9.figshare.28547696.v1 for 2021 samples, on figshare repository under accession code https://doi.org/10.6084/m9.figshare.13739086.v7 for 2017 mammal samples and on Dryad repository under accession code https://doi.org/10.5061/dryad.pvmcvdnmr for 2017 fish samples.

References

Altermatt, F., Carraro, L., Antonetti, M., Albouy, C., Zhang, Y., Lyet, A., Zhang, X., Pellissier, L., 2023. Quantifying biodiversity using eDNA from water bodies : general principles and recommendations for sampling designs. Environ. DNA 5 (4), 671–682. https://doi.org/10.1002/edn3.430.

Alvarenga, L.R.P., Pompeu, P.S., Leal, C.G., Hughes, R.M., Fagundes, D.C., Leitão, R.P., 2021. Land-use changes affect the functional structure of stream fish assemblages in the Brazilian savanna. Neotropical Ichthyology 19 (3), e210035. https://doi.org/10.1590/1982-0224-2021-0035.

Arantes, C.C., Winemiller, K.O., Petrere, M., Castello, L., Hess, L.L., Freitas, C.E.C., 2018. Relationships between forest cover and fish diversity in the Amazon River floodplain. J. Appl. Ecol. 55 (1), 386–395. https://doi.org/10.1111/1365-2664.12967.

Becker, J.J., Sandwell, D.T., Smith, W.H.F., Braud, J., Binder, B., Depner, J., Fabre, D., Factor, J., Ingalls, S., Kim, S.-H., Ladner, R., Marks, K., Nelson, S., Pharaoh, A., Trimmer, R., Von Rosenberg, J., Wallace, G., Weatherall, P., 2009. Global bathymetry and elevation data at 30 arc seconds resolution : SRTM30_PLUS. Mar. Geod. 32 (4), 355–371. https://doi.org/10.1080/01490410903297766.

Biggs, J., Ewald, N., Valentini, A., Gaboriaud, C., Dejean, T., Griffiths, R.A., Foster, J., Wilkinson, J.W., Arnell, A., Brotherton, P., Williams, P., Dunn, F., 2015. Using eDNA to develop a national citizen science-based monitoring programme for the great crested newt (Triturus cristatus). Biol. Conserv. 183, 19–28. https://doi.org/10.1016/j.biocon.2014.11.029.

Blackman, R., Couton, M., Keck, F., Kirschner, D., Carraro, L., Cereghetti, E., Perrelet, K., Bossart, R., Brantschen, J., Zhang, Y., Altermatt, F., 2024. Environmental DNA : the next chapter. Mol. Ecol. 33 (11), e17355. https://doi.org/10.1111/mec.17355.

Boyer, F., Mercier, C., Bonin, A., Le Bras, Y., Taberlet, P., Coissac, E., 2016. OBITOOLS : A UNIX -inspired software package for DNA metabarcoding. Mol. Ecol. Resour. 16 (1), 176–182. https://doi.org/10.1111/1755-0998.12428.

Brejão, G.L., Hoeinghaus, D.J., Pérez-Mayorga, M.A., Ferraz, S.F.B., Casatti, L., 2018. Threshold responses of Amazonian stream fishes to timing and extent of deforestation. Conserv. Biol. 32 (4), 860–871. https://doi.org/10.1111/cobi.13061.

Brooks, M., Bolker, B., Kristensen, K., Maechler, M., Magnusson, A., Skaug, H., Nielsen, A., Berg, C., & Van Bentham, K. (2017). *glmmTMB : Generalized Linear Mixed Models using Template Model Builder* (p. 1.1.10) [Jeu de données]. doi:10.32614/CRAN.package.glmmTMB.

Cantera, I., Cilleros, K., Valentini, A., Cerdan, A., Dejean, T., Iribar, A., Taberlet, P., Vigouroux, R., Brosse, S., 2019. Optimizing environmental DNA sampling effort for fish inventories in tropical streams and rivers. Sci. Rep. 9 (1), 3085. https://doi.org/10.1038/s41598-019-39399-5.

Cantera, I., Coutant, O., Jézéquel, C., Decotte, J.-B., Dejean, T., Iribar, A., Vigouroux, R., Valentini, A., Murienne, J., Brosse, S., 2022. Low level of anthropization linked to harsh vertebrate biodiversity declines in Amazonia. Nat. Commun. 13 (1), 3290. https://doi.org/10.1038/s41467-022-30842-2.

Cantera, I., Jézéquel, C., Dejean, T., Murienne, J., Vigouroux, R., Valentini, A., Brosse, S., 2023a. Deforestation strengthens environmental filtering and competitive exclusion in Neotropical streams and rivers. Proc. R. Soc. B Biol. Sci. 290 (2006), 20231130. https://doi.org/10.1098/rspb.2023.1130.

Cantera, I., Jézéquel, C., Dejean, T., Murienne, J., Vigouroux, R., Valentini, A., Brosse, S., 2023b. Functional responses to deforestation in fish communities inhabiting neotropical streams and rivers. Ecol. Process. 12 (1), 52. https://doi.org/10.1186/s13717-023-00463-8.

Carmona, C. P., Tamme, R., Pärtel, M., De Bello, F., Brosse, S., Capdevila, P., González-M., R., González-Suárez, M., Salguero-Gómez, R., Vásquez-Valderrama, M., & Toussaint, A. (2021). Erosion of global functional diversity across the tree of life. *Science* Advances, 7(13), eabf2675. doi:https://doi.org/10.1126/sciadv.abf2675.

Carraro, L., Blackman, R.C., Altermatt, F., 2023. Modelling environmental DNA transport in rivers reveals highly resolved spatio-temporal biodiversity patterns. Sci. Rep. 13 (1), 8854. https://doi.org/10.1038/s41598-023-35614-6.

Castello, L., Macedo, M.N., 2016. Large-scale degradation of Amazonian freshwater ecosystems. Glob. Chang. Biol. 22 (3), 990–1007. https://doi.org/10.1111/gcb.13173.

Chen, K., Olden, J.D., 2020. Threshold responses of riverine fish communities to land use conversion across regions of the world. Glob. Chang. Biol. 26 (9), 4952–4965. https://doi.org/10.1111/gcb.15251.

Cilleros, K., Valentini, A., Allard, L., Dejean, T., Etienne, R., Grenouillet, G., Iribar, A., Taberlet, P., Vigouroux, R., & Brosse, S. (2019). Unlocking biodiversity and conservation studies in high-diversity environments using environmental DNA (eDNA) : A test with Guianese freshwater fishes. Mol. Ecol. Resour., 19(1), 27–46. doi:https://doi.org/10.1111/1755-0998.12900.

Coutant, O., Cantera, I., Cilleros, K., Dejean, T., Valentini, A., Murienne, J., Brosse, S., 2020. Detecting fish assemblages with environmental DNA: does protocol matter ? Testing eDNA metabarcoding method robustness. Environ. DNA 3 (3), 619–630. https://doi.org/10.1002/edn3.158.

Coutant, O., Jézéquel, C., Mokany, K., Cantera, I., Covain, R., Valentini, A., Dejean, T., Brosse, S., Murienne, J., 2023. Environmental DNA reveals a mismatch between diversity facets of Amazonian fishes in response to contrasting geographical, environmental and anthropogenic effects. Glob. Chang. Biol. 29 (7), 1741–1758. https://doi.org/10.1111/gcb.16533.

Coutant, O., Richard-Hansen, C., de Thoisy, B., Decotte, J.B., Valentini, A., Dejean, T., Vigouroux, R., Murienne, J., Brosse, S., 2021. Amazonian Mammal Monitoring Using Aquatic Environmental DNA. Molecular Ecology Resources, March, pp. 1–14. https://doi.org/10.1111/1755-0998.13393.

Dale, V.H., Beyeler, S.C., 2001. Challenges in the development and use of ecological indicators. Ecol. Indic. 1 (1), 3–10. https://doi.org/10.1016/S1470-160X(01)00003-6.

De Barba, M., Miquel, C., Boyer, F., Mercier, C., Rioux, D., Coissac, E., Taberlet, P., 2014. DNA metabarcoding multiplexing and validation of data accuracy for diet assessment : application to omnivorous diet. Mol. Ecol. Resour. 14 (2), 306–323. https://doi.org/10.1111/1755-0998.12188.

De Thoisy, B., Brosse, S., Dubois, M.A., 2008. Assessment of large-vertebrate species richness and relative abundance in Neotropical forest using line-transect censuses : what is the minimal effort required? Biodivers. Conserv. 17 (11), 2627–2644. https://doi.org/10.1007/s10531-008-9337-0.

Dezécache, C., Faure, E., Gond, V., Salles, J.-M., Vieilledent, G., Hérault, B., 2017. Gold-rush in a forested El Dorado : deforestation leakages and the need for regional cooperation. Environ. Res. Lett. 12 (3), 034013. https://doi.org/10.1088/1748-9326/aa6082.

France, Météo, 2024. Données climatologiques de base—Mensuelles. https://meteo.data.gouv.fr/datasets/donnees-climatologiques-de-base-mensuelles/.

Freitas, P.V., Montag, L.F.A., Ilha, P., Torres, N.R., Maia, C., Deegan, L., Nascimento, A. T., Silva, K.D., 2021. Local effects of deforestation on stream fish assemblages in the amazon-savannah transitional area. Neotropical Ichthyology 19 (3), e210098. https://doi.org/10.1590/1982-0224-2021-0098.

Gallay, M., Martinez, J., Allo, S., Mora, A., Cochonneau, G., Gardel, A., Doudou, J., Sarrazin, M., Chow-Toun, F., Laraque, A., 2018. Impact of land degradation from mining activities on the sediment fluxes in two large rivers of French Guiana. Land Degrad. Dev. 29 (12), 4323–4336. https://doi.org/10.1002/ldr.3150.

Gonzalez, A., Cardinale, B.J., Allington, G.R.H., Byrnes, J., Arthur Endsley, K., Brown, D. G., Hooper, D.U., Isbell, F., O'Connor, M.I., Loreau, M., 2016. Estimating local biodiversity change : A critique of papers claiming no net loss of local diversity. Ecology 97 (8), 1949–1960. https://doi.org/10.1890/15-1759.1.

Gotelli, N.J., 2000. Null Model Analysis of Species Co-Occurrence Patterns, vol. 81 (9).

Hansen, M.C., Potapov, P.V., Moore, R., Hancher, M., Turubanova, S.A., Tyukavina, A., Thau, D., Stehman, S.V., Goetz, S.J., Loveland, T.R., Kommareddy, A., Egorov, A., Chini, L., Justice, C.O., Townshend, J.R.G., 2013. High-resolution global maps of 21st-century Forest cover change. Science 342 (6160), 850–853. https://doi.org/10.1126/science.1244693.

Harrison, J.B., Sunday, J.M., Rogers, S.M., 2019. Predicting the fate of eDNA in the environment and implications for studying biodiversity. Proc. R. Soc. B Biol. Sci. 286 (1915), 20191409. https://doi.org/10.1098/rspb.2019.1409.

Hartig, F., Lohse, L., 2022. DHARMa : residual diagnostics for hierarchical (multi-level / mixed) regression models (version 0.4.6) [Logiciel]. https://cran.r-project.org/web/packages/DHARMa/index.html.

INSEE, 2020. Population légale 2017. Retrieved from. *https://www.insee.fr*.

IPBES. (2019). *Summary for policymakers of the global assessment report on biodiversity and ecosystem services of the Intergovernmental Science-Policy Platform on Biodiversity and Ecosystem Services. S. Díaz, J. Settele, E. S. Brondízio E.S., H. T. Ngo, M. Guèze, J. Agard, A. Arneth, P. Balvanera, K. A. Brauman, S. H. M. Butchart, K. M. A. Chan, L. A. Garibaldi, K. Ichii, J. Liu, S. M. Subramanian, G. F. Midgley, P. Miloslavich, Z. Molnár, D. Obura, A. Pfaff, S. Polasky, A. Purvis, J. Razzaque, B. Reyers, R. Roy Chowdhury, Y. J. Shin, I. J. Visseren-Hamakers, K. J. Willis, and C. N. Zayas (eds.)* (p. 56). IPBES secretariat, Bonn, Germany.

Jones, K.E., Bielby, J., Cardillo, M., Fritz, S.A., O'Dell, J., Orme, C.D.L., Safi, K., Sechrest, W., Boakes, E.H., Carbone, C., Connolly, C., Cutts, M.J., Foster, J.K., Grenyer, R., Habib, M., Plaster, C.A., Price, S.A., Rigby, E.A., Rist, J., Purvis, A., 2009. PanTHERIA : A species-level database of life history, ecology, and geography of extant and recently extinct mammals: ecological archives E090-184. Ecology 90 (9), 2648. https://doi.org/10.1890/08-1494.1.

Keck, F., Blackman, R.C., Bossart, R., Brantschen, J., Couton, M., Hürlemann, S., Kirschner, D., Locher, N., Zhang, H., Altermatt, F., 2022. Meta-analysis shows both congruence and complementarity of DNA and eDNA metabarcoding to traditional methods for biological community assessment. Mol. Ecol. 31 (6), 1820–1835. https://doi.org/10.1111/mec.16364.

Kembel, S.W., Ackerly, D.D., Blomberg, S.P., Cornwell, W.K., Cowan, P.D., Helmus, M.R., Morlon, H., Webb, C.O., 2020. Picante : integrating phylogenies and ecology (version 1.8.2) [Logiciel]. https://cran.r-project.org/web/packages/picante/index.html.

Kocher, A., De Thoisy, B., Catzeflis, F., Huguin, M., Valière, S., Zinger, L., Bañuls, A., Murienne, J., 2017. Evaluation of short mitochondrial metabarcodes for the identification of Amazonian mammals. Methods Ecol. Evol. 8 (10), 1276–1283. https://doi.org/10.1111/2041-210X.12729.

Leal, C.G., Lennox, G.D., Ferraz, S.F.B., Ferreira, J., Gardner, T.A., Thomson, J.R., Berenguer, E., Lees, A.C., Hughes, R.M., Mac Nally, R., Aragão, L.E.O.C., de Brito, J. G., Castello, L., Garrett, R.D., Hamada, N., Juen, L., Leitão, R.P., Louzada, J., Morello, T.F., Barlow, J., 2020. Integrated terrestrial-freshwater planning doubles conservation of tropical aquatic species. Science 370 (6512), 117–121. https://doi.org/10.1126/science.aba7580.

Leitão, R.P., Zuanon, J., Mouillot, D., Leal, C.G., Hughes, R.M., Kaufmann, P.R., Villéger, S., Pompeu, P.S., Kasper, D., De Paula, F.R., Ferraz, S.F.B., Gardner, T.A., 2018. Disentangling the pathways of land use impacts on the functional structure of fish assemblages in Amazon streams. Ecography 41 (1), 219–232. https://doi.org/10.1111/ecog.02845.

Lüdecke, D., Makowski, D., Ben-Shachar, M. S., Patil, I., Waggoner, P., Wiernik, B. M., & Thériault, R. (2019). Performance : Assessment of Regression Models Performance (p. 0.13.0) [Jeu de données]. doi:10.32614/CRAN.package.performance.

Luo, M., Ji, Y., Warton, D., Yu, D.W., 2023. Extracting abundance information from DNA-based data. Mol. Ecol. Resour. 23 (1), 174–189. https://doi.org/10.1111/1755-0998.13703.

Lyet, A., Pellissier, L., Valentini, A., Dejean, T., Hehmeyer, A., Naidoo, R., 2021. eDNA sampled from stream networks correlates with camera trap detection rates of terrestrial mammals. Sci. Rep. 11 (1), 11362. https://doi.org/10.1038/s41598-021-90598-5.

MacConaill, L.E., Burns, R.T., Nag, A., Coleman, H.A., Slevin, M.K., Giorda, K., Light, M., Lai, K., Jarosz, M., McNeill, M.S., Ducar, M.D., Meyerson, M., Thorner, A.R., 2018. Unique, dual-indexed sequencing adapters with UMIs effectively eliminate index cross-talk and significantly improve sensitivity of massively parallel sequencing. BMC Genomics 19 (1), 30. https://doi.org/10.1186/s12864-017-4428-5.

Macher, T.-H., Schütz, R., Arle, J., Beermann, A.J., Koschorreck, J., Leese, F., 2021. Beyond fish eDNA metabarcoding : field replicates disproportionately improve the detection of stream associated vertebrate species. Metabarcoding and Metagenomics 5, e66557. https://doi.org/10.3897/mbmg.5.66557.

Magneville, C., cre, cph, Loiseau, N., Albouy, C., Casajus, N., Claverie, T., Escalas, A., Leprieur, F., Maire, E., Mouillot, D., & Villeger, S. (2024). *mFD : Compute and Illustrate the Multiple Facets of Functional Diversity* (Version 1.0.7) [Logiciel]. https://cran.r-project.org/web/packages/mFD/index.html.

Mathieu, C., Hermans, S.M., Lear, G., Buckley, T.R., Lee, K.C., Buckley, H.L., 2020. A systematic review of sources of variability and uncertainty in eDNA data for environmental monitoring. Front. Ecol. Evol. 8, 135. https://doi.org/10.3389/fevo.2020.00135.

Matthews, T. J., Triantis, K. A., Wayman, J. P., Martin, T. E., Hume, J. P., Cardoso, P., Faurby, S., Mendenhall, C. D., Dufour, P., Rigal, F., Cooke, R., Whittaker, R. J., Pigot, A. L., Thébaud, C., Jørgensen, M. W., Benavides, E., Soares, F. C., Ulrich, W., Kubota, Y., … Sayol, F. (2024). The Global Loss of Avian Functional and Phylogenetic Diversity from Anthropogenic Extinctions. *Science* (New York, N.Y.), vol. 386(6717), 55–60. doi:https://doi.org/10.1126/science.adk7898.

Mena, J.L., Yagui, H., Tejeda, V., Bonifaz, E., Bellemain, E., Valentini, A., Tobler, M.W., Sánchez-Vendizú, P., Lyet, A., 2021. Environmental DNA metabarcoding as a useful tool for evaluating terrestrial mammal diversity in tropical forests. Ecol. Appl. 31 (5), e02335. https://doi.org/10.1002/eap.2335.

Mouillot, D., Graham, N.A.J., Villéger, S., Mason, N.W.H., Bellwood, D.R., 2013. A functional approach reveals community responses to disturbances. Trends Ecol. Evol. 28 (3), 167–177. https://doi.org/10.1016/j.tree.2012.10.004.

Myhrvold, N.P., Baldridge, E., Chan, B., Sivam, D., Freeman, D.L., Ernest, S.K.M., 2015. An amniote life-history database to perform comparative analyses with birds, mammals, and reptiles. Ecology 96 (11), 3109. https://doi.org/10.1890/15-0846R.1.

Newton, J.P., Allentoft, M.E., Bateman, P.W., van der Heyde, M., Nevill, P., 2025. Targeting terrestrial vertebrates with eDNA : trends, perspectives, and considerations for sampling. Environ. DNA 7 (1), e70056. https://doi.org/10.1002/edn3.70056.

Penone, C., Davidson, A.D., Shoemaker, K.T., Di Marco, M., Rondinini, C., Brooks, T.M., Young, B.E., Graham, C.H., Costa, G.C., 2014. Imputation of missing data in life-history trait datasets : which approach performs the best? Methods Ecol. Evol. 5 (9), 961–970. https://doi.org/10.1111/2041-210X.12232.

Pinheiro, J., Bates, D., & R Core Team. (1999). Nlme : Linear and Nonlinear Mixed Effects Models (p. 3.1-166) [Jeu de données]. doi:10.32614/CRAN.package.nlme.

Pont, D., 2024. Predicting downstream transport distance of fish eDNA in lotic environments. Mol. Ecol. Resour. 24 (4), e13934. https://doi.org/10.1111/1755-0998.13934.

Pringle, C., 2001. Hydrologic connectivity and the management of biological reserves : A global perspective. Ecol. Appl. 11 (4), 981–998. https://doi.org/10.1890/1051-0761(2001)011[0981,HCATMO]2.0.CO;2.

Riaz, T., Shehzad, W., Viari, A., Pompanon, F., Taberlet, P., Coissac, E., 2011. ecoPrimers : inference of new DNA barcode markers from whole genome sequence analysis. Nucleic Acids Res. 39 (21), e145. https://doi.org/10.1093/nar/gkr732.

Ripple, W.J., Wolf, C., Newsome, T.M., Hoffmann, M., Wirsing, A.J., McCauley, D.J., 2017. Extinction risk is most acute for the world's largest and smallest vertebrates. Proc. Natl. Acad. Sci. 114 (40), 10678–10683. https://doi.org/10.1073/pnas.1702078114.

Rourke, M., Fowler, A., Hughes, J., Broadhurst, M., Dibattista, J., Fielder, D., Wilkes Walburn, J., Furlan, E., 2021. Environmental DNA (eDNA) as a tool for assessing fish biomass : A review of approaches and future considerations for resource surveys. Environ. DNA 2022, 9–33. https://doi.org/10.1002/edn3.185.

Sales, N.G., McKenzie, M.B., Drake, J., Harper, L.R., Browett, S.S., Coscia, I., Wangensteen, O.S., Baillie, C., Bryce, E., Dawson, D.A., Ochu, E., Hänfling, B., Lawson Handley, L., Mariani, S., Lambin, X., Sutherland, C., McDevitt, A.D., 2020. Fishing for mammals : landscape-level monitoring of terrestrial and semi-aquatic communities using eDNA from riverine systems. J. Appl. Ecol. 57 (4), 707–716. https://doi.org/10.1111/1365-2664.13592.

Schenekar, T., 2023. The current state of eDNA research in freshwater ecosystems : are we shifting from the developmental phase to standard application in biomonitoring? Hydrobiologia 850 (6), 1263–1282. https://doi.org/10.1007/s10750-022-04891-z.

Schnell, I.B., Bohmann, K., Gilbert, M.T.P., 2015. Tag jumps illuminated – reducing sequence-to-sample misidentifications in metabarcoding studies. Mol. Ecol. Resour. 15 (6), 1289–1303. https://doi.org/10.1111/1755-0998.12402.

Silva, N.C.D.S., Soares, B.E., Teresa, F.B., Caramaschi, É.P., Albrecht, M.P., 2022. Fish functional diversity is less impacted by mining than fish taxonomic richness in an Amazonian stream system. Aquat. Ecol. 56 (3), 815–827. https://doi.org/10.1007/s10452-022-09946-w.

Stewart, K.A., 2019. Understanding the effects of biotic and abiotic factors on sources of aquatic environmental DNA. Biodivers. Conserv. 28 (5), 983–1001. https://doi.org/10.1007/s10531-019-01709-8.

Su, G., Logez, M., Xu, J., Tao, S., Villéger, S., Brosse, S., 2021. Human impacts on global freshwater fish biodiversity. Science 371 (6531), 835–838. https://doi.org/10.1126/science.abd3369.

Sullivan, S.M.P., Manning, D.W.P., 2019. Aquatic–terrestrial linkages as complex systems : insights and advances from network models. Freshwater Science 38 (4), 936–945. https://doi.org/10.1086/706071.

Swenson, N. G. (2014). Null Models. In N. G. Swenson (Éd.), Functional and Phylogenetic Ecology in R (p. 109–146). Springer. doi:https://doi.org/10.1007/978-1-4614-9542-0_6.

Taberlet, P., Bonin, A., Zinger, L., Coissac, É., 2018. Environmental DNA : For Biodiversity Research and Monitoring. For Biodiversity Research and Monitoring, In *Environmental DNA*. https://doi.org/10.1093/oso/9780198767220.001.0001.

Teichert, N., Lepage, M., Lobry, J., 2018. Beyond classic ecological assessment : the use of functional indices to indicate fish assemblages sensitivity to human disturbance in estuaries. Sci. Total Environ. 639, 465–475. https://doi.org/10.1016/j.scitotenv.2018.05.179.

Tickner, D., Opperman, J.J., Abell, R., Acreman, M., Arthington, A.H., Bunn, S.E., Cooke, S.J., Dalton, J., Darwall, W., Edwards, G., Harrison, I., Hughes, K., Jones, T., Leclère, D., Lynch, A.J., Leonard, P., McClain, M.E., Muruven, D., Olden, J.D., Young, L., 2020. Bending the curve of global freshwater biodiversity loss : an emergency recovery plan. Bioscience 70 (4), 330–342. https://doi.org/10.1093/biosci/biaa002.

Valentini, A., Taberlet, P., Miaud, C., Civade, R., Herder, J., Thomsen, P.F., Bellemain, E., Besnard, A., Coissac, E., Boyer, F., Gaboriaud, C., Jean, P., Poulet, N., Roset, N., Copp, G.H., Geniez, P., Pont, D., Argillier, C., Baudoin, J., Dejean, T., 2016. Next-generation monitoring of aquatic biodiversity using environmental DNA metabarcoding. Mol. Ecol. 25 (4), 929–942. https://doi.org/10.1111/mec.13428.

Van Driessche, C., Everts, T., Neyrinck, S., Brys, R., 2023. Experimental assessment of downstream environmental DNA patterns under variable fish biomass and river discharge rates. Environ. DNA 5 (1), 102–116. https://doi.org/10.1002/edn3.361.

Villéger, S., Brosse, S., Mouchet, M., Mouillot, D., Vanni, M.J., 2017. Functional ecology of fish : current approaches and future challenges. Aquat. Sci. 79 (4), 783–801. https://doi.org/10.1007/s00027-017-0546-z.

Villéger, S., Mason, N.W.H., Mouillot, D., 2008. New multidimensional functional diversity indices for A multifaceted framework in functional ecology. Ecology 89 (8), 2290–2301. https://doi.org/10.1890/07-1206.1.

Watson, J.E.M., Evans, T., Venter, O., Williams, B., Tulloch, A., Stewart, C., Thompson, I., Ray, J.C., Murray, K., Salazar, A., McAlpine, C., Potapov, P., Walston, J., Robinson, J.G., Painter, M., Wilkie, D., Filardi, C., Laurance, W.F., Houghton, R.A., Lindenmayer, D., 2018. The exceptional value of intact forest ecosystems. Nature Ecology and Evolution 2 (4), 599–610. https://doi.org/10.1038/s41559-018-0490-x.

Watson, J.E.M., Shanahan, D.F., Di Marco, M., Allan, J., Laurance, W.F., Sanderson, E. W., Mackey, B., Venter, O., 2016. Catastrophic declines in wilderness areas undermine global environment targets. Curr. Biol. 26 (21), 2929–2934. https://doi.org/10.1016/j.cub.2016.08.049.

WWF, 2024. Living Planet Report 2024—A System in Peril. Gland, Switzerland. https://www.worldwildlife.org/publications/2024-living-planet-report.

Yao, M., Zhang, S., Lu, Q., Chen, X., Zhang, S., Kong, Y., Zhao, J., 2022. Fishing for fish environmental DNA : ecological applications, methodological considerations, surveying designs, and ways forward. Mol. Ecol. 31 (20), 5132–5164. https://doi.org/10.1111/mec.16659.

Zhang, H., Mächler, E., Morsdorf, F., Niklaus, P.A., Schaepman, M.E., Altermatt, F., 2023. A spatial fingerprint of land-water linkage of biodiversity uncovered by remote sensing and environmental DNA. Sci. Total Environ. 867, 161365. https://doi.org/10.1016/j.scitotenv.2022.161365.